Speed Gradient Approach to Longitudinal Control of Heavy-Duty Vehicles Equipped With Variable Compression Brake

Maria Druzhinina, Anna G. Stefanopoulou, *Member, IEEE*, and Lasse Moklegaard

***Abstract*—This paper considers a longitudinal speed control problem for heavy-duty vehicles equipped with variable compression brake. The use of compression brake reduces the wear of the conventional friction brakes, and it is, thus, a preferred way of controlling the vehicle speed during a steady descent or noncritical braking maneuvers. To perform more aggressive (critical) braking maneuvers or control vehicle speed during large changes in the grade, the compression brake must be coordinated with gear ratio adjustments and friction brakes. In this paper we develop nonlinear controllers that accomplish both noncritical and critical maneuvers. We also show how distance constraints from other vehicles in traffic may be included. The design technique is based on the speed-gradient (SG) approach, whereby the control action is chosen in the maximum descent direction for a scalar goal function. The nominal goal function is selected to address the speed regulation objective and, then, it is appropriately modified by barrier functions to handle the critical maneuver requirements. Two ways to handle the uncertainty in the road grade are discussed: through the use of an integral action of the SG controller for constant (but unknown) grades, and through the use of an added differential action for varying grades.**

***Index Terms*—Automotive, braking, compression brake, heavy-duty vehicles, Lyapunov methods, nonlinear control, speed control.**

I. Introduction

THE LAST ten years have witnessed a significant increase in the efficiency and operational speed of the heavy-duty vehicle (HDV) powertrains. This transformation is primarily achieved by using lightweight materials, and by reducing aerodynamic drag and friction losses that are, actually, the main natural retarding sources for HDVs. Thus, while the fuel efficiency and acceleration performance have improved, at the same time the vehicle natural retarding capability have decreased, thereby limiting the deceleration performance of HDVs. The main vehicle retarders, namely, the service/friction brakes (friction pads on the wheels) can provide a sufficient retarding power to decelerate the vehicle to a desired speed. They may not, however, be used *continuously* to maintain the desired speed because of the potential damage/loss of performance due to overheating and increased wear [1]. The current recommended practice to brake on a downgrade by intermittent application of the service brakes (or *snubbing*) rather than continuous application (or *dragging*) exemplifies these limitations [2]. Wear and overheating not only reduce the steady-state authority of the friction brakes but also cause large parameter variations [3]. Adaptive algorithms have been developed in [4] to address unpredictable changes in brake model parameters. Recent work [5] shows that nonsmooth estimation and adaptation techniques can be used to achieve reasonable brake friction force control. The presence of delays associated with the pneumatic or the hydraulic subsystem in the friction brake actuators imposes additional difficulties in using friction brakes for the longitudinal control of HDVs. These difficulties in autonomous HDVs can be mitigated by using aggressive prediction algorithms [6]. The prediction algorithms, however, assume accurate knowledge of the delays and do not perform well during a totally uncertain brake maneuver. Thus, augmenting the braking performance of HDVs with auxiliary retarding mechanisms with consistent magnitude and unlimited duration is increasingly important in order to integrate HDVs into the advanced transit and highway systems [7], [8].

A very promising retarding mechanism that satisfies the low maintenance and weight-to-power ratio requirements is the engine compression brake that relies on converting the turbocharged diesel engine, that powers the HDV, into a compressor that absorbs kinetic energy from the crankshaft [9], [10]. The compression brake increases the overall decelerating capability of the vehicle and can potentially be used as a sole decelerating actuator during low deceleration requests and combined with the friction brakes during high deceleration requests. Therefore, the application and intensity of the friction brakes can be reduced resulting in a significant decrease in the vehicle maintenance costs.

In this paper, we concentrate on the longitudinal control problem using variable compression braking to its maximum extent in an effort to minimize the use of conventional friction brake and, hence, the friction brake wear. Subsequently, we consider two types of braking maneuvers that are classified as critical and noncritical. The noncritical braking maneuvers reflect the requirement of maintaining the desired vehicle speed during a long descent down a (possibly varying) grade but when there are no critical requirements on time of response (such as during collision avoidance). During noncritical maneuvers the compression brake can be used as the only decelerating actuator, possibly combined with gear ratio adjustments to handle large grade changes. On the other hand, critical

Manuscript received August 19, 2000. Manuscript received in final form August 24, 2001. Recommended by Associate Editor K. Hunt. This work was supported in part by the California Department of Transportation through the California PATH Program under MOU 372 and MOU 393; matching funds are provided by Mack Trucks, Inc.

M. Druzhinina and A. G. Stefanopoulou are with the Department of Mechanical Engineering, University of Michigan, Ann Arbor, MI 48109 USA.

L. Moklegaard is with the Department of Mechanical and Environmental Engineering, University of California, Santa Barbara, CA 93106 USA.

Publisher Item Identifier S 1063-6536(02)00334-2.

braking maneuvers require aggressive braking action with both compression and friction brakes, where friction brake is used to supplement the compression braking capability. We develop nonlinear controllers that accomplish both critical and noncritical maneuvers and we address distance constraints from other vehicles in traffic. The controllers are designed using the speed-gradient (SG) methodology [11], [12]. This is a general technique for controlling nonlinear systems through an appropriate selection and dynamic minimization of a scalar goal function. The nominal goal function is selected to address the speed regulation objective. Motivated by robotics obstacle avoidance applications [13], barrier functions are then added to the nominal goal function to handle critical braking requirements. The controller is designed to provide the decrease of the goal function along the trajectories of the system. The local closed-loop stability is verified analytically by checking the achievability condition. It is shown that the controller is guaranteed to have a large region of attraction covering a very reasonable interval of initial values for the vehicle speed. Two approaches to compensate for an uncertainty in the road grade are investigated. One approach relies on the integral action of the speed-gradient proportional-plus-integral (SG-PI) controller. This controller can compensate for unknown constant (or slowly varying) grade and other uncertainties, including the uncertainty in the aerodynamic coefficient. An alternative approach is based on the derivative action of the speed-gradient proportional-plus-derivative (SG-PD) controller, that can compensate for fast varying grade essentially by estimating the torque due to the unknown grade. The above controllers are appropriately modified to provide coordination between the compression brake, friction brake and the gear ratio adjustment. Specifically, to handle large changes in the grade during noncritical maneuvers, a scheme that coordinates the compression brake with the gear ratio adjustment is described. To handle critical maneuvers another scheme that coordinates the compression brake with the friction brake is also developed. The friction brake is engaged only when it is necessary to supplement the compression brake.

This paper is organized as follows. The operating principles of compression braking mechanism are reviewed in Section II. The model for longitudinal vehicle speed control is described in Section III. In Section IV, we review the necessary results of the SG methodology that is used to develop nonlinear controllers in this paper. In Section V, we apply the methodology to the development and evaluation of the SG-PI controller, followed by the development and evaluation of the SG-PD controller. The scheme that coordinates the compression brake with the gear ratio adjustments is described at the end of that section. In Section VI, we address critical maneuvers. In particular, aggressive braking and speed regulation under traffic constraints are considered. The closed-loop performance is demonstrated through simulations. Finally, concluding remarks are made in Section VII.

II. Variable Compression Braking Mechanism

The engine compression brake is a retarder that enhances braking capability by altering the conventional gas exchange process in the cylinders of the engine and effectively converting the turbocharged diesel engine, that powers the HDV, into a compressor that absorbs kinetic energy from the crankshaft [9]. During the compression braking the fuel injection and combustion are inhibited. Through the work done by the pistons, using the crankshaft kinetic energy, the air in the cylinder is compressed in the compression stroke. At the end of the compression stroke, close to the time when fuel injection usually takes place, the exhaust valve opens dissipating the energy stored in the compressed air into the exhaust manifold. We call the secondary opening of the exhaust valve when the air is released into the exhaust as brake valve opening (BVO) (or braking event), and we refer to the corresponding timing of the exhaust valve opening as BVO timing, u_{cb}. Specifically, we define u_{cb} as the number of crank angle degrees from the top-dead-center (TDC) at the beginning of the power stroke to the opening of the brake valve, as shown in Fig. 1. Due to geometric constraints, the exhaust valve lift profile is considerably different for the exhaust and brake events. Note that in the absence of BVO essentially all the potential energy stored in the compressed air will return to the wheels by the downward piston motion. With the secondary exhaust valve opening, however, the kinetic energy absorbed during the compression stroke can be dissipated into the exhaust manifold. In conventional compression braking mechanisms, currently available in the market, the activation of the brake valve events is based on the mechanical link between the crankshaft and the camshaft. As a result, the brake valve opens at fixed degrees with respect to piston motion and only a finite number of possible braking torque values can be achieved for a given engine speed. The number of possible discrete torque values depends on the number of cylinders activated under compression mode. In order to satisfy the stringent requirements of HDV following and other applications in intelligent transportation systems, compression braking using a continuously variable BVO is desirable. It allows smooth braking torque variations for a given speed, and thus, full integration with the conventional friction brakes. Due to the expected benefits, many engine manufacturers are intensively pursuing the development of appropriate hardware [14]. In this type of compression braking, the valves are activated by variable exhaust camshaft phasing actuators so that is why continuously variable BVO is possible.

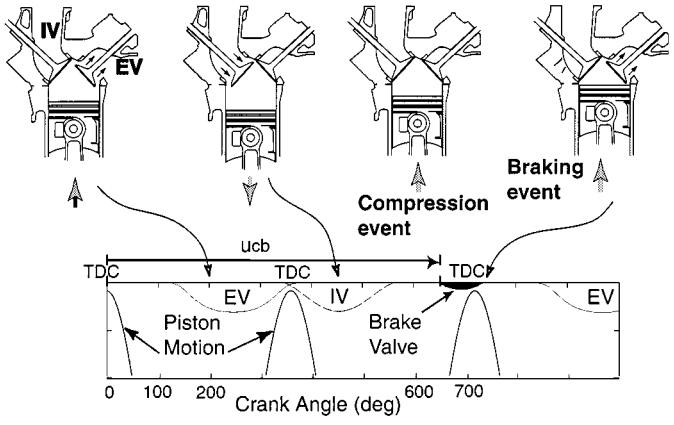

Fig. 1. Lift profiles for exhaust, intake, and brake events.

That is the type of compression braking mechanism that we focus on in the paper.

III. Vehicle Dynamics Model

Consider the vehicle operation during a driving maneuver on a descending grade with β degrees inclination ($\beta = 0$ corresponds to no inclination, $\beta > 0$ corresponds to a descending grade). It is assumed that during the descent, the engine is not fueled and is operated in the compression braking mode.

A lumped parameter model approximation is used to describe the vehicle longitudinal dynamics during compression braking. For fixed gear operation the engine crankshaft rotational speed, ω, is expressed by

$$J_t\dot{\omega} = T_{cb} + r_g(F_\beta - F_{qdr} + F_{fb}) \tag{1}$$

where $J_t = Mr_g^2 + J_e$ is the total vehicle inertia reflected to the engine shaft, J_e is the engine crankshaft inertia, M is the mass of the vehicle (depends on the mass of payload). The total gear ratio, r_g, is given by $r_g = r_\omega/g_t g_{fd}$, where r_ω is the wheel diameter, g_t is the transmission gear ratio, g_{fd} is the final drive gear ratio. F_{qdr} is the quadratic resistive force (primarily, force due to aerodynamic resistance, but we also include friction resistive terms)

$$F_{qdr} = C_q v^2 = C_q r_g^2 \omega^2$$

where $C_q = (C_d A\rho/2) + C_f$ is the quadratic resistive coefficient, C_d is the aerodynamic drag coefficient, ρ is ambient air-density, A is the frontal area of the vehicle and C_f is the friction coefficient. F_β is the force due to road grade (β) and the rolling resistance of the road(μ)

$$F_\beta = -\mu g M\cos\beta + Mg\sin\beta$$

where g is the acceleration due to gravity. F_{fb} is the force on the vehicle due to application of the conventional friction brake (negative during friction braking), and T_{cb} is the engine torque applied to the crankshaft (negative during compression braking). The engine speed ω is proportional to the vehicle speed, v, i.e.,

$$v = \omega r_g \tag{2}$$

as long as the gear ratio remains constant.

In [15] we developed a detailed crank angle-based model to predict the compression braking torque. Applying numerical model order reduction techniques to this model a set of low-order model approximations was developed in [16]. To facilitate the analysis and control design here we approximate the compression brake torque on the crankshaft, T_{cb}, as a static nonlinear function of the engine speed, ω, and the timing of BVO, u_{cb} (see Fig. 2)

$$T_{cb}(\omega, u_{cb}) = \alpha_0 + \alpha_1\omega + \alpha_2 u_{cb} + \alpha_3 u_{cb}\omega. \tag{3}$$

The timing of brake valve opening, u_{cb}, is the input signal to the compression braking mechanism and is physically limited to the range $u_{cb}^{\min} = 620°$ to $u_{cb}^{\max} = 680°$ after TDC. These BVO limits translate into limits on the torque $T_{cb}^{\min}(\omega) = T_{cb}(u_{cb}^{\max}, \omega)$, $T_{cb}^{\max}(\omega) = T_{cb}(u_{cb}^{\min}, \omega)$.

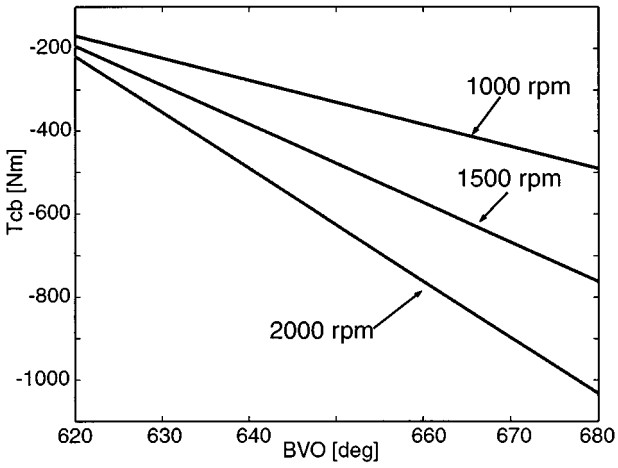

Fig. 2. Static nonlinear compression braking torque map.

The speed control problem is to ensure that the vehicle speed $v(t)$ tracks the desired reference vehicle speed v_d as the truck proceeds down the descending grade, i.e., $v \to v_d$. Since the engine rotational speed $\omega(t)$ is related to the vehicle speed by (2), this ensures that $\omega \to \omega_d$, where $\omega_d = v_d/r_g$ is the desired engine speed. Additionally, we assume that the braking with the compression brake is preferable to avoid the friction brake wear. Thus the friction brake is used only when absolutely necessary.

The controller is designed using the SG methodology [12] reviewed in Section IV. This is a general technique for controlling nonlinear systems through an appropriate selection and dynamic minimization of a scalar goal function. In our case, we select a nominal goal function Q to reflect the speed regulation objective, i.e.,

$$Q = \frac{J_t\gamma_0}{2}(v - v_d)^2 \geq 0, \qquad \gamma_0 > 0. \tag{4}$$

Taking into account the relation (2), the goal function can be also written as follows:

$$Q = \frac{J_t\gamma}{2}(\omega - \omega_d)^2 \geq 0, \qquad \gamma = \gamma_0/r_g^2 > 0. \tag{5}$$

IV. Speed-Gradient Methodology

In this section we review the necessary results of the SG control methodology [11], [12]. Consider a nonlinear system of the form

$$\dot{x} = f(x) + g(x)u \tag{6}$$

where $x \in R^n$ is the state vector, $u \in R^m$ is the control input vector, $f(x)$ and $g(x)$ are continuously differentiable vector-functions.

The control design objective is to stabilize to a desired equilibrium $x = x_d$ [that satisfies $f(x_d) + g(x_d)u_d = 0$ for some $u_d \in R^m$] while at the same time shaping the transient response via the minimization of the following scalar goal function:

$$Q(x(t)) \to 0, \qquad \text{as} \quad t \to \infty \tag{7}$$

where $Q(x)$ is assumed to be twice continuously differentiable function that satisfies $Q(x) \geq 0$, $Q(x_d) = 0$. The function Q

may, for example, represent a weighted sum of the squares of the deviations of the different components of x from the corresponding components of x_d.

We first present an intuitive argument leading to the derivation of the SG controller. Consider the evolution of $Q(x(t))$ over a sufficiently small time interval $[t, t+\Delta t]$. Then, the objective of minimizing Q can be restated as

$$Q(t+\Delta t) \approx Q(t) + \xi(x(t), u(t))\Delta t \to \min$$

where the function $\xi(x, u)$ is determined as a time derivative of $Q(x)$ along the trajectories of the system (6) (i.e., the speed of change of Q)

$$\xi(x, u) = \dot{Q} = \frac{\partial Q}{\partial x}(f(x) + g(x)u).$$

To prevent large control excursions from the desired steady-state value, u_d, we can augment a control penalty and consider the minimization of the following function for $\Pi > 0$:

$$Q(t) + \xi(x(t), u)\Delta t + \frac{1}{2}(u-u_d)^{\mathrm{T}}\left(\frac{\Pi}{\Delta t}\right)^{-1}(u-u_d).$$

Since $\xi(x(t), u)$ is affine in u the minimizer is obtained by setting the gradient with respect to u to zero. This leads to the controller

$$u(t) = u_d - \Pi\Psi(x) \tag{8}$$

where Ψ is the gradient of the "speed" $\dot{Q} = \xi(x(t), u)$ with respect to u:

$$\Psi(x) \triangleq \nabla_u \xi(x(t), u) = \left(\frac{\partial Q}{\partial x}\, g(x)\right)^{\mathrm{T}}. \tag{9}$$

This controller is referred to as the speed-gradient proportional (SG-P) controller. One can also augment a penalty on the control increment and consider the minimization of the following function for $\Gamma > 0$:

$$Q(t) + \xi(x(t), u)\Delta t + \tfrac{1}{2}(u(t)-u(t-\Delta t))^{\mathrm{T}}\Gamma^{-1}(u(t)-u(t-\Delta t)).$$

This results in the speed-gradient integral (SG-I) controller

$$\dot{u}(t) \approx \frac{u(t)-u(t-\Delta t)}{\Delta t} = -\Gamma\nabla_u\xi(x(t), u) = -\Gamma\Psi(x). \tag{10}$$

A more general class of controllers that are used in this paper are the SG-PI controllers of the form

$$u(t) = u_d - \Pi\Psi(x(t)) - \Gamma\int_0^t \Psi(x(s))\, ds \tag{11}$$

where $\Pi = \Pi^T > 0$ and $\Gamma = \Gamma^T > 0$ are symmetric positive definite matrices (usually diagonal). In general, there is no guarantee that the controller (11) results in the stable closed-loop system and is robust to disturbances. However, one may provide stability and robustness properties under some sufficient stability conditions as reviewed next.

We start by rewriting the control law (11) in a more convenient equivalent form

$$u = u_d - \Pi\Psi(x) + \theta, \qquad \dot{\theta} = -\Gamma\Psi(x) \tag{12}$$

where θ is the integrator state. Let us consider the following Lyapunov function:

$$V(x, \theta) = Q(x) + \tfrac{1}{2}\theta^{\mathrm{T}}\Gamma^{-1}\theta \geq 0 \tag{13}$$

and calculate its time-derivative along the trajectories of the closed-loop system (6), (12)

$$\begin{aligned}\dot{V} &= \frac{\partial Q}{\partial x}(f(x) + g(x)u) + \theta^{\mathrm{T}}\Gamma^{-1}\dot{\theta} \\ &= \frac{\partial Q}{\partial x}(f(x) + g(x)u_d) - \Psi^{\mathrm{T}}(x)\Pi\Psi(x).\end{aligned} \tag{14}$$

Now, let us define the following sets:

$$\Upsilon_C \triangleq \{x\colon Q(x) \leq C\}, \quad \Omega_C \triangleq \{(x, \theta)\colon V(x, \theta) \leq C\}$$

and suppose that the so called *achievability condition* holds

$$\frac{\partial Q}{\partial x}(f(x) + g(x)u_d) \leq -\rho(Q(x)) \qquad \text{for all } x \in \Upsilon_C \tag{15}$$

where ρ is a continuously differentiable function that satisfies $\rho(0) = 0$, $\rho(z) > 0$ if $z \neq 0$.

Since the achievability condition holds for $x(t) \in \Upsilon_C$, then $\dot{V}(t) \leq 0$ as long as $x(t) \in \Upsilon_C$. Assume that the initial condition at time $t = 0$ is $(x(0), \theta(0))$ such that $(x(0), \theta(0)) \in \Omega_C$, i.e., $x(0)$, $\theta(0)$ satisfy the following inequalities:

$$\begin{aligned} Q(x(0)) &\leq C\cdot\lambda, \\ \tfrac{1}{2}\theta(0)^{\mathrm{T}}\Gamma^{-1}\theta(0) &\leq C\cdot(1-\lambda), \qquad 0 \leq \lambda \leq 1.\end{aligned}$$

Then, for all t, $V(x(t), \theta(t)) \leq V(x(0), \theta(0)) \leq C$ and $Q(x(t)) \leq C$ so that the achievability condition holds on the trajectory $x(t, x(0), \theta(0)), \theta(t, x(0), \theta(0))$. Thus, $V(x(t), \theta(t))$ is nonincreasing function of time and $V(x(t), \theta(t), Q(x(t))$ are bounded. The closed-loop system trajectories $x(t), \theta(t)$ are bounded as well due to radial unboundness of $Q(x)$. Then, taking into account boundedness of $f(x)$ and $g(x)$ on any compact set we get that $\dot{x}(t)$ is bounded and, therefore, $x(t)$ is uniformly continuous in t. Further since $\rho(Q)$ is continuous in Q, then $\rho(Q(x(t)))$ is uniformly continuous in t. Moreover, $\int_0^\infty \rho(Q(x(s)))\, ds < \infty$ from (14). The Barbalat's lemma can now be applied to show that $Q(x(t)) \to 0$ as $t \to \infty$. Additionally, let us assume that $Q(x_d) = 0$, $Q(x) > 0$ for $x \neq x_d$. Then, it follows that $x \to x_d$.

Hence, the above facts demonstrate the following result.

Theorem 1: Consider the SG-PI controller (12) applied to the system (6). Assume that the achievability condition (15) holds for all $x \in \Upsilon_C$. Then for all initial conditions $(x(0), \theta(0))$ in Ω_C the closed-loop trajectories satisfy $\lim_{t\to\infty} Q(x(t)) = 0$. Moreover, if $Q(x)$ satisfies $Q(x_d) = 0$ and $Q(x) > 0$ for $x \neq x_d$, the closed-loop system meets the control objective $\lim_{t\to\infty} x(t) = x_d$.

Remark 1: The set $\Omega_C = \{(x, \theta)\colon Q(x) + (1/2)\theta^{\mathrm{T}}\Gamma^{-1}\theta \leq C\}$ is a region of attraction of the equilibrium $(x_d, 0)$. Typically, $\theta(0)$ is set to zero, and then all initial states $x(0) \in \Upsilon_C = \{x\colon$

$Q(x) \le C\}$ are guaranteed to be recoverable by the controller (12).

Remark 2: The same result can be proved for the SG-P controller (8). Indeed, in this case the Lyapunov function V coincides with the objective function $Q(x)$ and the region of attraction is the set Υ_C.

The vector u_d in the SG-P controller (8) and SG-PI controller (12) can be interpreted as an ideal feedforward term: $f(x_d)+g(x_d)u_d = 0$. Due to plant parameter variations, u_d may be unknown. However, in the case of the SG-PI controller (since the controller employs an integral action), we expect some robustness properties to disturbances that are additive to the plant input. Let w be an unknown constant additive disturbance affecting the plant input. Using w to represent the error in the feedforward term, the controller then can be viewed as applying an erroneous feedforward $\tilde{u}_d$ in the form $\tilde{u}_d = u_d + w$. Thus, the SG-PI controller can be represented as

$$\begin{aligned} u &= u_d - \Pi\Psi(x) + \theta + w \\ \dot{\theta} &= -\Gamma\Psi(x) \end{aligned} \tag{16}$$

where θ can be interpreted as an estimate of $-w$. The desirable property $\theta(t) \to -w$, and, therefore, $\tilde{u}_d + \theta(t) \to u_d$ means that the integrator state corrects for the error in the feedforward asymptotically.

Consider the following Lyapunov function:

$$\tilde{V}(x, \theta) = Q(x) + \tfrac{1}{2}(\theta + w)^{\mathrm{T}}\Gamma^{-1}(\theta + w) \tag{17}$$

and define the set

$$\tilde{\Omega}_C \triangleq \left\{(x, \theta)\colon \tilde{V}(x, \theta) \le C\right\}.$$

Theorem 2: Consider the SG-PI controller (16) applied to the system (6). Assume that the achievability condition (15) holds for all $x \in \Upsilon_C$. Then for all the initial conditions $(x(0), \theta(0))$ in $\tilde{\Omega}_C$ the closed-loop trajectories satisfy: $\lim_{t\to\infty} Q(x(t)) = 0$. Moreover, if $Q(x)$ satisfies $Q(x_d) = 0$ and $Q(x) > 0$ for $x \ne x_d$, the closed-loop system meets the control objective $\lim_{t\to\infty} x(t) = x_d$. If, furthermore, the $n \times m$ matrix $g(x_d)$ has a full column rank m, then $\lim_{t\to\infty} \theta(t) = -w$, $\lim_{t\to\infty}(\tilde{u}_d + \theta(t)) = u_d$.

Proof: The proof of the theorem is based on calculating the time-derivative of the Lyapunov function (17) along the trajectories of the closed-loop system (6), (16):

$$\dot{V} = \frac{\partial Q}{\partial x}\left(f(x) + g(x)u_d\right) - \Psi^{\mathrm{T}}(x)\Pi\Psi(x).$$

Since the achievability condition holds for $x(t) \in \Upsilon_C$, then $\dot{V}(t) \le 0$ as long as $x(t) \in \Upsilon_C$. Suppose that the initial condition at time $t = 0$ is $x(0)$ such that

$$Q(x(0)) \le c \cdot \lambda, \qquad 0 \le \lambda \le 1, \tag{18}$$

while $\theta(0)$ (the initial "estimate" of $-w$) yields

$$\tfrac{1}{2}(\theta(0) + w)^{\mathrm{T}}\Gamma^{-1}(\theta(0) + w) \le C \cdot (1 - \lambda). \tag{19}$$

Then, for all t, $V(x(t), \theta(t)) \le V(x(0), \theta(0)) \le C$ and $Q(x(t)) \le C$ so that the achievability condition holds on the trajectory $x(t, x(0), \theta(0))$, $\theta(t, x(0), \theta(0))$. Applying the Barbalat's lemma to

$$\dot{V}(t) \le -\rho(Q(x)) - \Psi^{\mathrm{T}}(x)\Pi\Psi(x) \le 0$$

one can prove that

$$\lim_{t\to\infty} \Psi(x(t)) = 0, \qquad \lim_{t\to\infty} Q(x(t)) = 0.$$

Moreover, if $Q(x)$ satisfies $Q(x_d) = 0$ and $Q(x) > 0$ for $x \ne x_d$, then $\lim_{t\to\infty} x(t) = x_d$. The fact that $\Psi(t) \to 0$, $Q(t) \to 0$, in general, does not guarantee that $\theta(t) \to -w$. Additional analysis is needed to establish this convergence. The convergence $\theta \to -w$ can be assured if the $n \times m$ matrix $g(x_d)$ has a full column rank. To show this we apply the Barbalat's lemma to $\dot{x}$, to obtain $\dot{x} \to 0$. From the closed-loop system equations

$$\dot{x} = \left(f(x) + g(x)u_d\right) - g(x)\Pi\Psi(x) + g(x)(\theta + w)$$

and $\Psi(x) \to 0$, $x \to x_d$ it follows that $g(x_d)(\theta(t) + w) \to 0$ and, hence, $\theta(t) \to -w$. ∎

Remark 3: The requirement of twice continuous differentiability of Q is only needed to guarantee that $\dot{Q}$ is uniformly continuous. The latter property allows us to apply Barbalat's lemma to prove convergence. It might be, however, technically difficult to use a twice continuously differentiable goal function (e.g., see Section V). In the case when Q does not satisfy this requirement, one should check the uniform continuity of $\dot{Q}$ via a direct argument.

Remark 4: The set $\tilde{\Omega}_C = \{(x, \theta)\colon Q(x) + (1/2)(\theta + w)^{\mathrm{T}}\Gamma^{-1}(\theta + w) \le C\}$ describes the set of initial conditions for which the closed-loop system trajectories are assured to meet the control objective (7). Although it is advantageous to have an initial estimate of $-w$, $\theta(0)$, as close as possible to $-w$, we typically set $\theta(0)$ to zero, because w is unknown. Then, the set of initial states $x(0)$ that are guaranteed to be recoverable by the controller (12), decreases when w increases.

Remark 5: To check the achievability condition (15) the following procedure is used. Assume that

$$\Upsilon_C = \{x\colon Q(x) \le C\}$$

for some $C > 0$ is a compact set with x_d in its interior and $Q(x) > 0$ if $x \ne x_d$, $Q(x_d) = 0$. We need to find a value of $\tilde{C}$ such that for all $x \in \Upsilon_{\tilde{C}} = \{x\colon Q(x) \le \tilde{C}\}$ the strong achievability condition

$$\dot{Q}(x, u_d) = \frac{\partial Q}{\partial x}\left(f(x) + g(x)u_d\right) \le -\rho Q(x) \tag{20}$$

where $\rho > 0$, holds. Essentially, ρ is a low bound on a rate of convergence of $Q(x(t))$ to zero on the trajectories of the open-loop system. Let us define the following function:

$$\kappa(C) \triangleq \max_{\Upsilon_C}\left(\frac{\dot{Q}(x, u_d)}{Q(x)}\right). \tag{21}$$

Note that $\kappa(C)$, in general, may take an infinite value since $Q(x_d) = 0$. On the other hand, $\dot{Q}(x_d, u_d) = 0$ and, hence, $\dot{Q}/Q$

may have a removable singularity at zero and we can, therefore, set

$$\dot{Q}(x_d, u_d)/Q(x_d) = \lim_{\|x\| \to x_d} \frac{\dot{Q}(x, u_d)}{Q(x)}.$$

In this case $\kappa(C)$ takes a finite value due to the compactness of Υ_C. The case that $\dot{Q}/Q$ has a removable singularity at x_d is, actually, rather usual in many applications. Moreover, $\kappa(C)$ is nondecreasing in C. The value of $\kappa(C)$ can be calculated using numerical optimization. From the graph of $\kappa(C)$ we may be able to specify $\tilde{C} > 0$ such that $\kappa(C) < 0$ for all $C \leq \tilde{C}$. Then, $\dot{Q}(x, u_d) \leq -\rho Q(x)$ as long as $Q(x) \leq \tilde{C}$, i.e., the strong achievability condition (20) holds.

Remark 6: We emphasize that achievability conditions are only sufficient stability conditions; the actual domain of attraction may be much larger than the sets Ω_C and $\tilde{\Omega}_C$. These stability conditions, however, place no restriction on the controller gains Π and Γ as long as they are positive definite matrices and, therefore, allow a considerable freedom in the selection of the controller.

Remark 7: The speed-gradient methodology is related to other constructive nonlinear design techniques, for example, those based on control Lyapunov function (CLF) methods and L_gV-techniques [17]. For affine in control systems, the differences are mainly in the approach: Q is selected by the designer to capture the performance objectives in the SG approach; Q is constructed as a CLF in the other methodologies. The strength of SG approach is in the strong linkage between control objectives and the selection of the goal function Q. In another application [18], this strength has been explored to shape the transient response of multiinput–multioutput automotive system. The weakness of SG approach is that if achievability conditions with the particular function Q do not hold the procedures to modify Q are not readily available. Note that the achievability conditions are only sufficient (see Remark 6) and the stability may be verified by other procedures.

V. Speed Control During Noncritical Maneuvers

In this section, we develop nonlinear SG controllers that accomplish noncritical braking maneuvers during a long descent down a grade. Recall that during noncritical maneuvers the time necessary to achieve the desired speed is not critical. This is a frequent situation, for example, when collision avoidance requirements are not a defining factor for the maneuver. To sustain the desired vehicle speed during a steady descent, we use compression brake only. However, we do consider large road grade changes and we account for compression brake saturation. To handle these large grade changes, the compression brake must be coordinated with gear changes. In the sequel, we first develop a SG-PI controller for compression braking that ensures robustness to a constant (or slowly varying) uncertainty in the grade. To handle more general time-varying grades, an estimator for the torque on the vehicle due to the unknown grade is combined with the SG controller. Finally, we develop the coordinated controller for the compression brake and gear ratio.

A. Control Design

The control design is based on the vehicle model with compression brake

$$J_t\dot{\omega} = \alpha_0 + \alpha_1\omega + (\alpha_2 + \alpha_3\omega)u_{cb} - C_q r_g^3\omega^2 + r_g F_\beta \quad (22)$$

where the timing of brake valve opening, u_{cb}, is the control input. We first rearrange the model (22) as follows:

$$J_t\dot{\omega} = \alpha_0 + \alpha_1\omega + (\alpha_2 + \alpha_3\omega)u_{cb} - C_q r_g^3(\omega - \omega_d)(\omega + \omega_d) + TQ$$

where $TQ = r_g F_\beta - r_g^3 C_q \omega_d^2$ is assumed to be a known function. In accordance with SG method, we calculate the time derivative of the goal function (5) along the trajectories of (22) and the derivative of $\dot{Q}$ with respect to u_{cb} ("speed-gradient"):

$$\nabla_{u_{cb}}\dot{Q} = \gamma(\omega - \omega_d)(\alpha_2 + \alpha_3\omega).$$

Then the SG-PI control has the following form:

$$u_{cb} = u_d - k_p\nabla_{u_{cb}}\dot{Q}(\omega) - k_i\int_0^t \nabla_{u_{cb}}\dot{Q}(\omega(s))\,ds \quad (23)$$

where $k_p > 0$, $k_i > 0$ are the controller gains and u_d is the feedforward of desired value for the input

$$u_d = \frac{-\alpha_0 - \alpha_1\omega_d - TQ}{\alpha_2 + \alpha_3\omega_d}. \quad (24)$$

The control law (23) can be interpreted as a traditional PI controller but with *nonlinear* gains which depend on engine speed ω. This form of controller allows to cover a large range of vehicle operating conditions that include gear changes and different engine speeds, without the need to recalibrate controller gains. The feedforward term (24) depends on road grade β and aerodynamic coefficient that are usually unknown. However, as shown in Section IV, the implementation of the SG-PI controller (23) is possible without knowing precisely the value of u_d, due to the integral action.

Since the sign of the total vehicle inertia J_t is always positive, we can include J_t into the goal function $Q \geq 0$ and, therefore, render the feedback portion of the control law (23) independent of the vehicle load. If J_t were not included into Q, the controller gains would be lowered as J_t increases—an undesirable effect. On the other hand, including J_t^2 into Q results in controller gains being multiplied by J_t that helps to provide consistent vehicle transient response irrespective of vehicle mass. The resulting controller may, however, require large control action to achieve the consistent vehicle speed transient response if the vehicle mass is large. Furthermore, the value of J_t may not be precisely known, unless an on-line mass estimation approach combined with controller gain adaptation is pursued [19]. Thus using J_t as a multiplier in the goal function Q was a reasonable tradeoff. Note that even if J_t is not accurately known, the controller (23) remains robust as far as local stability is concerned.

B. Verifying Achievability Condition

The verification of the closed-loop stability is done in accordance with the procedure in Remark 4. Specifically, let us consider a set

$$\Upsilon_C = \{\omega\colon Q(\omega) \leq C\} = \{\omega\colon (\omega - \omega_d)^2 \leq 2C/J_t\gamma\}$$

for some $C > 0$ and find the following function:

$$k(C) = \max_{\omega \in \Upsilon_C} \left(\frac{\dot{Q}(\omega, u_d)}{Q(\omega)} \right).$$

First, let us calculate $\dot{Q}$ under the assumption that $u = u_d$. After some algebraic manipulations, we obtain

$$\dot{Q}(\omega, u_d) = -\gamma(\omega - \omega_d)^2 \left(-\alpha_1 - \alpha_3 u_d + C_q r_g^3(\omega + \omega_d)\right).$$

Then

$$\frac{\dot{Q}(\omega, u_d)}{Q(\omega)} = -\frac{2C_q r_g^3}{J_t}(\omega + G), \quad G = \omega_d - \frac{\alpha_3 u_d + \alpha_1}{C_q r_g^3}. \quad (25)$$

It can be verified numerically that G is always positive for all physically feasible values of the grade β, mass M and desired engine speed ω_d. Note that (25) reaches its maximum value on the compact set Υ_C at $\omega = \omega_d - \sqrt{2C/J_t\gamma}$, i.e.,

$$k(C) = -\frac{2C_q r_g^3}{J_t}\left(\omega_d - \sqrt{2C/J_t\gamma} + G\right). \quad (26)$$

Therefore, we can guarantee that $\kappa(C) < 0$ for all $C \leq \tilde{C}$, where $\tilde{C}$ is any positive number such that

$$\tilde{C} < \frac{J_t\gamma}{2}(\omega_d + G)^2. \quad (27)$$

This implies that the strong achievability condition (20) holds for all $\omega \in \Upsilon_{\tilde{C}} = \{\omega\colon Q(\omega) \leq \tilde{C}\}$. Since G is positive, we can select $\tilde{C} = (J_t\gamma/2)\omega_d^2$. Then, the set of initial states $\omega(0)$ in $\Upsilon_{\tilde{C}} = \{\omega\colon (\omega - \omega_d)^2 \leq \omega_d^2\}$ is guaranteed to be recoverable by the controller (23) with $\theta(0) = 0$ provided that TQ and u_d are known (see remark 4 for the case when TQ and u_d are unknown). This implies that the controller (23) with any positive gains $k_p > 0$, $k_i > 0$ is guaranteed to have a large region of attraction covering a very reasonable interval of initial values for the vehicle speed that corresponds to the engine speed interval of $[0, 2\omega_d]$.

C. Controller Performance During Small Changes in the Grade

We tested through simulations the operation of the SG-PI controller during a noncritical maneuver. In this maneuver the compression brake alone is used to sustain the desired vehicle speed during a long descent, while the friction brake remains inactive. The vehicle mass is 20 000 kg, and the value of desired vehicle speed $v_d = 8.78$ m/s (or 31.6 km/h) corresponds to desired engine speed $\omega_d = 1500$ r/min in the gear number seven. Figs. 3 and 4 illustrate the SG-PI controller response to unmeasured changes in the road grade. The feedforward term u_d was calculated assuming a grade of $\beta = 2.5°$ while the actual grade changes from 1.8 to 4.2° during simulation. The unknown grade creates an unmeasured disturbance which is additive to the control input. As shown in Theorem 2, the SG-PI controller rejects this type of disturbances since the integral state corrects for the error in the feedforward u_d. It can be seen that although the timing of BVO, u_{cb}, saturates during the initial transients the antiwindup compensation that we used in combination with our controller preserves good speed regulation performance. Note

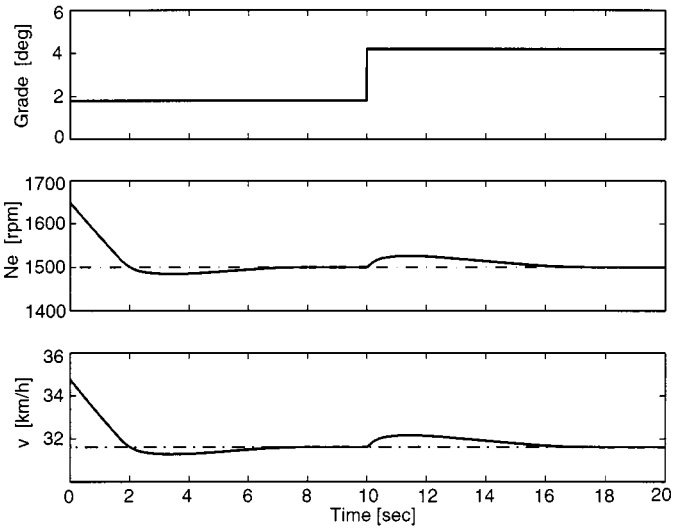

Fig. 3. Controller responses to disturbance in road grade from 1.8 to 4.2°: trajectories of grade, engine speed, and vehicle speed. The desired engine and vehicle speeds are shown by the dashed line.

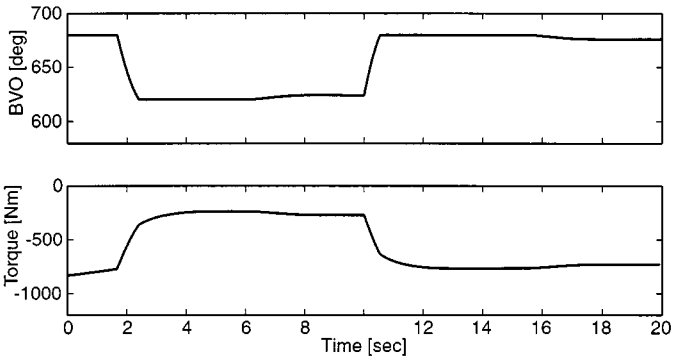

Fig. 4. Controller responses to disturbance in road grade from 1.8 to 4.2°: trajectories of BVO timing and compression torque.

that although our control design was based on the static model of the compression braking torque as a function of u_{cb} and engine speed, the compression braking torque dynamics were included in the simulation model used for controller testing.

D. Time-Varying Disturbance Rejection

In Section IV we have shown that the SG-PI controller rejects unknown disturbances that are additive to the control input. In our application they may include unmeasured changes in road grade. However, these disturbances must be constant (or slowly varying) for the integral action to compensate for them. In order to reject more general, unmeasured fast varying disturbances induced by road grade changes, an alternative approach can be pursued.

We treat the deviation from the nominal force due to grade as an unknown time-varying disturbance, i.e., the system (22) has the following form:

$$J_t\dot{\omega} = T_{cb} - r_g F_{qdr} + r_g(F_\beta^{nom} + \triangle F_\beta) \quad (28)$$

where $\triangle F_\beta = F_\beta - F_\beta^{nom}$ is treated as an unknown function of time. It is reasonable to assume that the unknown function $\triangle F_\beta$ and its derivative are bounded.

We, first, rearrange the model (28) as follows:

$$J_t\dot{\omega} = T_{cb} - C_q r_g^3(\omega-\omega_d)(\omega+\omega_d) + TQ_{nom} + W \quad (29)$$

where $TQ_{nom} = r_g F_\beta^{nom} - r_g^3 C_q \omega_d^2$ is a known function, while $W(t) = r_g \triangle F_\beta(t)$ is an unknown function of time, bounded together with its derivative, i.e.,

$$|W(t)| \le L, \qquad \left|\dot{W}(t)\right| \le \tilde{L}$$

for some constant $L > 0$, $\tilde{L} > 0$. Our approach is to estimate the unknown disturbance torque, $W(t)$, with an observer that provides an estimate, $\hat{W}$, and then combine the observer with SG-P controller, i.e.,

$$u_{cb} = u_d - k_p \nabla_{u_{cb}} \dot{Q}(\omega) - \frac{\hat{W}}{\alpha_2 + \alpha_3\omega} \quad (30)$$

where $\nabla_{u_{cb}}\dot{Q} = \gamma(\omega-\omega_d)(\alpha_2+\alpha_3\omega)$, $k_p > 0$, is the controller gain and the feedforward term u_d is selected as before to balance the nominal system at the desired equilibrium

$$u_d = \frac{-\alpha_0 - \alpha_1\omega_d - TQ_{nom}}{\alpha_2 + \alpha_3\omega_d}. \quad (31)$$

The observer for $W(t)$ can be defined using the method of [20]. We first define an observer for ω via

$$J_t\dot{\hat{\omega}} = T_{cb} - C_q r_g^3(\omega-\omega_d)(\omega+\omega_d) + TQ_{nom} + \hat{W}$$

where $\hat{W}$ is chosen to force $\hat{\omega}$ to track ω. Indeed, if $\hat{\omega}$ tracks ω, we can expect that $\hat{W}$ will approximately track W. Specifically, we may use $\hat{W} = k_{obs}J_t(\omega-\hat{\omega})$, where $k_{obs} > 0$ is an observer gain. Denoting $\epsilon = k_{obs}J_t\hat{\omega}$ we have the following form for $\hat{W}$:

$$\hat{W} = k_{obs}J_t\omega - \epsilon \quad (32)$$

where ϵ is the solution of the following differential equation:

$$\dot{\epsilon} = -k_{obs}\left(-T_{cb} + C_q r_g^3(\omega-\omega_d)(\omega+\omega_d) - TQ_{nom} - \hat{W}\right). \quad (33)$$

Denoting the estimation error by $e = \hat{W} - W$, we consider the Lyapunov function $V_{obs} = (1/2)e^2$. Calculating the time derivative of V_{obs} along the solutions of the system (29)–(33), we obtain

$$\dot{V}_{obs} \le -k_{obs}e^2 + \tilde{L}e \le -k_{obs}V_{obs} + \frac{\tilde{L}^2}{2k_{obs}}.$$

This implies that the estimation error $e(t)$ can be made arbitrarily small by amplifying the observer gain k_{obs}. Moreover, $e(t) \to 0$ if $W = const$, for any $k_{obs} > 0$.

We now consider the following Lyapunov function:

$$V_1(\omega, e) = Q + V_{obs} = \frac{J_t\gamma}{2}(\omega-\omega_d)^2 + \frac{1}{2}e^2$$

and calculate its time derivative along the solutions of the system (29)–(33)

$$\dot{V}_1 \le \dot{Q}(\omega, u_d)|_{W=0} - k_p\gamma^2(\omega-\omega_d)^2(\alpha_2+\alpha_3\omega)^2 - \gamma(\omega-\omega_d)e - k_{obs}\frac{e^2}{2} + \frac{\tilde{L}^2}{2k_{obs}}$$

where

$$\dot{Q}(\omega, u_d)|_{W=0} = -\gamma(\omega-\omega_d)^2\left(-\alpha_1 - \alpha_3 u_d + C_q r_g^3(\omega+\omega_d)\right).$$

As previously, we can guarantee that the achievability condition $\dot{Q}(\omega, u_d)|_{W=0} \le -\rho Q(\omega)$ holds for some $\rho > 0$ and all $\omega \in \Upsilon_{\tilde{C}} = \{\omega: Q(\omega) \le \tilde{C}\}$, where $\tilde{C} < (J_t\gamma/2)(\omega_d+G)^2$, is given by (27) with u_d calculated by (31).

If $\omega \in \Upsilon_{\tilde{C}}$, we obtain

$$\dot{V}_1 \le -\rho Q(\omega) - k_p\left(\gamma(\omega-\omega_d)(\alpha_2+\alpha_3\omega) + \frac{e}{2k_p(\alpha_2+\alpha_3\omega)}\right)^2 - \frac{1}{2}e^2\left(k_{obs} - \frac{1}{2k_p^2(\alpha_2+\alpha_3\omega)^2}\right) + \frac{\tilde{L}^2}{2k_{obs}}.$$

Suppose that the initial condition at time $t = 0$ is $(\omega(0), e(0))$ such that $V_1(\omega(0), e(0)) = Q(\omega(0)) + (1/2)e(0)^2 \le \tilde{C}$. From the analysis of the expression for $\dot{V}_1$ it can be shown that for k_{obs} sufficiently large the set $\Omega_{\tilde{C}} = \{(\omega, e): V_1(\omega, e) \le \tilde{C}\}$ becomes positively invariant, and, in particular, $Q(\omega(t)) \le V_1(\omega(t), e(t)) \le \tilde{C}$ for all $t \ge 0$ so that $\omega(t) \in \Upsilon_{\tilde{C}}$ for all $t \ge 0$. Furthermore, both $e(t)$ and $Q(\omega(t))$ can be made ultimately bounded in a given (arbitrarily small) neighborhood of the origin. Consequently, the initial accuracy of grade estimation is important to guarantee a large domain of attraction for our controller. Note that the bandwidth of the observer, k_{obs}, does not depend on the magnitude of $W(t)$, only on the bound for the time-rate of change of W, $\tilde{L}$. Furthermore, stability conditions place no restriction on the controller gain k_p as long as it is positive.

The observer (32) and (33) and TQ_{nom} depend on the aerodynamic coefficient C_q. For the SG-PI controller (30), the robustness to uncertainties in C_q was assured as these uncertainties only affected the feedforward term u_d. If the value of C_q is not accurately known the observer-based design (30)–(33) can use the best estimate of C_q, C_q^{nom}.

The controller (30)–(33) is referred to as SG-PD controller. This controller relies on the fast differential action to estimate and compensate the unmeasured disturbances, as opposed to the slow integral action of the SG-PI controller. Hence, one can expect much faster disturbance rejection with SG-PD controller in response to a grade change.

The operation of the SG-PD controller is tested through simulations during a noncritical maneuver, when the unknown road grade creates unmeasured time-varying disturbances from 2 to 4° (see Figs. 5 and 6). The implementation of the controller is done assuming the nominal grade value of 3°. The responses show that the disturbances due to grade essentially do not affect the vehicle speed.

E. Coordination With Gear

Since the braking torque T_{cb} is limited, in steady-state the compression brake can only support a certain range of vehicle speeds, v_d (or ω_d), for a given grade, β. Or, stated differently, given the desired vehicle velocity, v_d, we can only drive down a

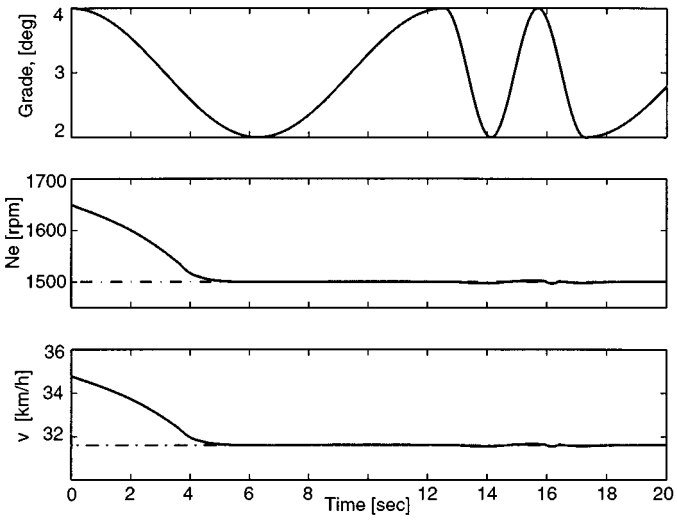

Fig. 5. Controller responses to time-varying disturbance in road grade from 2 to 4°: trajectories of grade, engine speed, and vehicle speed. The desired engine and vehicle speeds are shown by the dashed line.

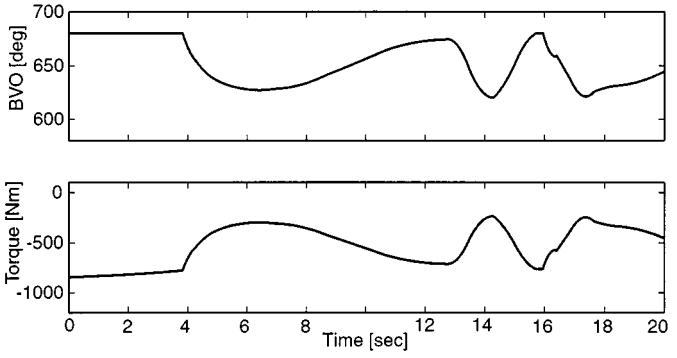

Fig. 6. Controller responses to time-varying disturbance in road grade from 2 to 4°: trajectories of BVO timing and compression braking torque.

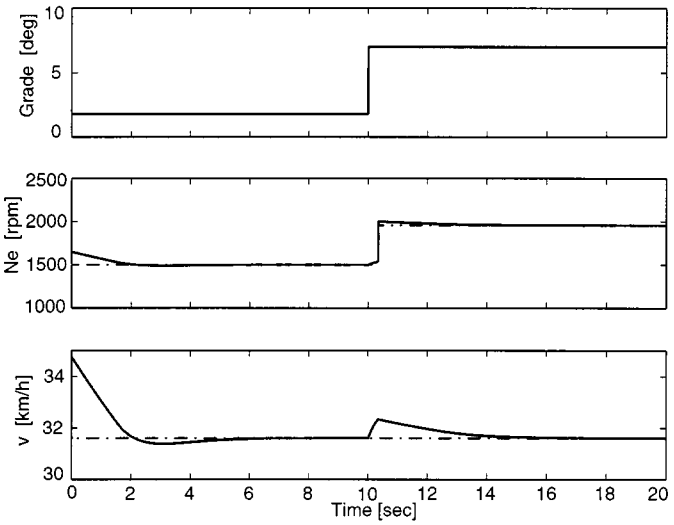

Fig. 7. Controller responses to a disturbance due to road grade change from 1.8 to 7°: trajectories of grade, engine speed, and vehicle speed. The desired engine and vehicle speed are shown by the dashed lines.

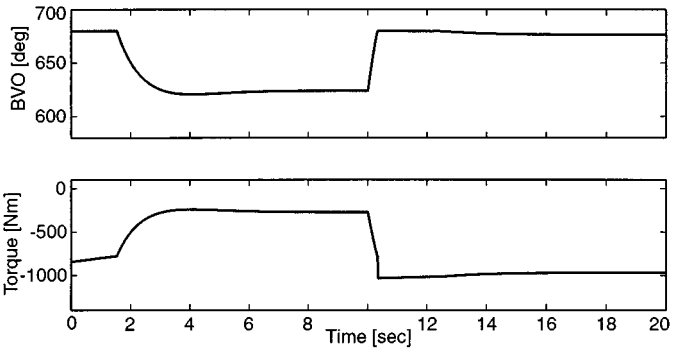

Fig. 8. Controller responses to disturbance in road grade from 1.8 to 7°: trajectories of gear ratio, BVO timing, and compression torque.

hill of a grade that falls within a certain range. To calculate this range, consider the steady-state balance of forces (or torques)

$$-T_{cb}/r_g + F_{qdr}(v,\, r_g) = F_\beta(M,\, \beta).$$

Given desired velocity v_d, gear ratio r_g and vehicle mass M, the determination of feasible grade range $\beta_{\min}$, $\beta_{\max}$ is an elementary root-finding problem:

$$-\mu g M\cos\beta_{\min} + Mg\sin\beta_{\min} = -T_{cb}^{\max}(v_d)r_g^{-1} + C_q v_d^2$$
$$-\mu g M\cos\beta_{\max} + Mg\sin\beta_{\max} = -T_{cb}^{\min}(v_d)r_g^{-1} + C_q v_d^2.$$

In the driving scenario, shown in Fig. 3, the feasible values for the road grade are within the range $\beta_{\min} = 1.62°$, $\beta_{\max} = 4.37°$. Therefore, for given vehicle mass and gear ratio the resulting compression brake is capable to support the desired speed v_d during the maneuver on a descending grade with inclination from 1.8 to 4.2°. However, if we operated on a grade β that exceeds the maximum value $\beta_{\max}$, the compression brake would not be able to support the desired velocity v_d under the same values of the mass and gear ratio. In this case we need to switch the gear number to a lower one (downshift) in order to increase the braking capability. The gear switching can be done by the following rule: we downshift from the gear number k to the gear number $k-1$ if the timing of BVO u_{cb} saturates at the upper limit, (i.e., $u_{cb} = u_{cb}^{\max}$) and the speed fails to decrease, i.e., $\dot\omega > 0$. If the gear $(k-1)$ is not sufficient (i.e., still $u_{cb} = u_{cb}^{\max}$ and $\dot\omega > 0$) we downshift to gear number $(k-2)$, etc. Note that in this scenario it can happen that there exists no gear ratio which would be able to guarantee the desired speed v_d for given grade β within the allowable range of engine speed, $\omega_{\min} \le \omega \le \omega_{\max}$, where $\omega_{\min} = 600$ r/min, $\omega_{\max} = 2100$ r/min. In this case we need to activate the friction brake to supplement the lack of compression braking torque. A similar procedure is used for the upshifting based on the condition $u_{cb} = u_{cb}^{\min}$ and $\dot\omega < 0$.

Figs. 7 and 8 illustrate the driving maneuver on a descending grade which changes from 1.8 to 7°. Initially we operate on gear seven, but in order to handle the large variation in the grade, we switch the gear number seven to the gear number six to increase our compression braking capability. The switch takes place at $t = 10$ s and implies the change in the desired engine speed. The value of desired vehicle speed $v_d = 8.78$ m/s (or 31.6 km/h) corresponds to desired engine speed $\omega_d = 1500$ r/min in the gear seven and $\omega_d = 1955$ r/min in the gear six.

VI. Speed Control During Critical Maneuvers

In this section we address maneuvers that require aggressive braking as in cases of collision avoidance. We call these maneuvers critical maneuvers because the time necessary to achieve the desired speed is important. The control design for critical maneuvers is based on the SG approach with the goal function appropriately modified by barrier functions to take into account the critical driving requirements. As can be seen from Section V, the compression brake coordinated with gear ratio control can be potentially used as the sole decelerating actuator without the assistance of friction brakes during noncritical maneuvers. However, to perform critical maneuvers, the friction brakes may be required.

A. Coordination With Friction Brake

The conventional friction brake force on the wheel F_{fb} can be considered as a nonlinear and uncertain function of the pneumatic friction brake actuator temperature and of the friction brake control signal. Recall that the braking with the compression brake is preferable, because we want to preserve the friction brake. Hence, we use the friction brake only when absolutely necessary. Specifically, if u_{cb} saturates, (i.e., $u_{cb} > u_{cb}^{\max}$ or $u_{cb} < u_{cb}^{\min}$) we calculate the torque deficit

$$\Delta TQ_{cb} = TQ_{cb}(\omega, u_{cb}) - TQ_{cb}(\omega, sat(u_{cb}))$$

and deliver it with the friction brake, $F_{fb} = \Delta TQ_{cb}/r_g$. Having made this convention, it is sufficient to consider the compression brake only with the idea that any extra braking effort required during the critical maneuver will be supplemented by the friction brake, according to the expression that we gave.

Remark 8: Although our control design and analysis does not treat friction brake actuator dynamics or uncertainties, we take them into account in all of our simulations. Specifically, we used 0.2 s as the time constant of the friction brake actuator [21] and show that the control schemes maintain speed regulation without serious degradation in performance.

B. Aggressive Braking

In addition to speed regulation it is important, here, to induce aggressive braking maneuvers when the difference between the current vehicle velocity, v, and the desired one, v_d, is sufficiently large, i.e., when $|v - v_d|$ exceeds a given number $\varepsilon_1 > 0$. Assuming that the gear ratio r_g remains constant, the aggressive braking is needed when

$$|\omega - \omega_d| \geq \varepsilon, \qquad \text{where } \varepsilon = \varepsilon_1/r_g, \quad \omega_d = v_d/r_g.$$

To capture the new requirement, the new goal function Q_1 has to include the nominal goal function $Q = (J_t\gamma/2)(\omega - \omega_d)^2$ and a smooth barrier function Φ_1 which is zero when the speed error $|\omega - \omega_d|$ is smaller than ε and is monotonically and rapidly increasing when the speed error is larger than ε (see Fig. 9)

$$Q_1 = \frac{J_t\gamma}{2}(\omega - \omega_d)^2 + \frac{J_t\gamma_1}{3}\Phi_1(\omega - \omega_d) \geq 0, \qquad \gamma_1 > 0$$

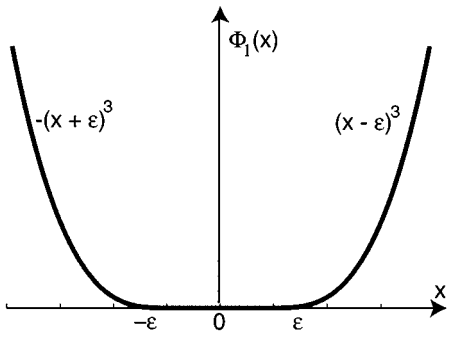

Fig. 9. Barrier function for aggressive braking maneuver.

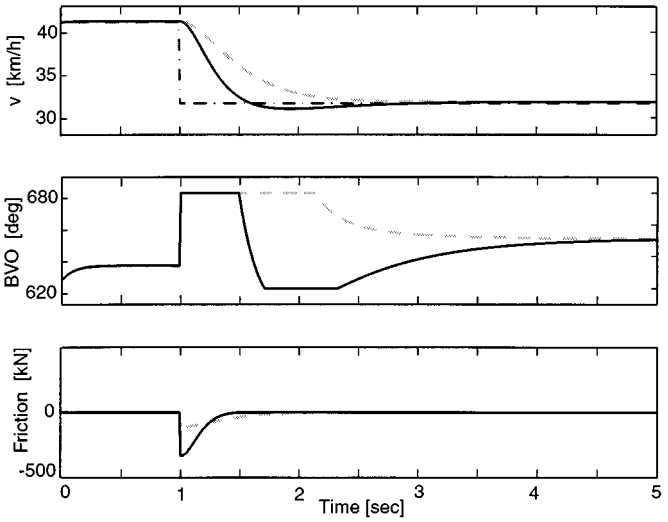

Fig. 10. The engine speed, vehicle speed, BVO timing, and friction force during aggressive control action (solid lines) and nominal control action (dashed lines). The desired engine and vehicle speed are shown by dash-dotted lines.

where

$$\Phi_1(\omega - \omega_d) = \begin{cases} 0, & \text{if } \omega - \omega_d \leq \varepsilon \\ (\omega - \omega_d - \varepsilon)^3, & \text{if } \omega - \omega_d > \varepsilon \\ -(\omega - \omega_d + \varepsilon)^3, & \text{if } \omega - \omega_d < -\varepsilon. \end{cases}$$

If the speed error falls outside the acceptable range $[-\varepsilon \quad \varepsilon]$ then Φ_1 takes a large value and forces the controller to respond rapidly. Thus, this control design ensures that normally the speed control is accomplished with the compression brake only. If we need to brake suddenly the barrier function amplifies the braking action and potentially causes the friction brake to engage. In this critical maneuver both the compression brake and friction brake are coordinated to decelerate rapidly.

Remark 9: A similar longitudinal speed control design which allows fast compensation for large errors in speed was achieved in [22] by introducing a signed-quadratic (Q) term into the PI controller.

Fig. 10 illustrates the critical driving scenario with aggressive braking. The value of $\varepsilon_1 = 0.29$ m/sc (or 1.05 km/h) corresponds to $\varepsilon = 50$ r/min in the gear number seven. Here we compare the engine and vehicle speed during aggressive control action with the engine and vehicle speed during nominal control action (without the barrier function). As can be seen,

the response of the controller with the barrier function is much faster than that of the nominal design.

C. Speed Regulation Under Traffic Constraints

We next study a problem when in addition to speed regulation we want to avoid any collisions between our vehicle and the leading vehicle. It means that we want to maintain the desired vehicle speed and, additionally, ensure a sufficient distance between our vehicle and the vehicle in front of us. This is an important driving scenario in automated highway systems (AHS) (see [3] and [22]–[24],)

Let s be the position of our truck as it goes down the hill, so that $\dot{s} = v$, and s_l be the position of a vehicle in front of ours (leading vehicle) as it goes down the hill. The objective of collision avoidance is then to always ensure that the separation distance (in seconds of travel) does not fall below a given number $\delta_1 \geq 0$, i.e.,

$$\left| \frac{s - s_l}{v} \right| \geq \delta_1. \tag{34}$$

As in previous section, here we assume that the gear ratio r_g remains constant. Therefore, the objective (34) can be restated as $|(s-s_l)/\omega| \geq \delta$, where $\delta = \delta_1/r_g$ and the new goal function Q_2, which captures the new requirement (34) will include the nominal goal function $Q = (J_t\gamma/2)(\omega - \omega_d)^2$ and a smooth barrier function Φ_2 that penalizes the small headway between the trucks in seconds, i.e.,

$$Q_2 = \frac{J_t\gamma}{2}(\omega - \omega_d)^2 + J_t\gamma_2\Phi_2\left(\frac{s - s_l}{\omega}\right) \geq 0, \qquad \gamma_2 > 0$$

where Φ_2 has to be zero when $|(s - s_l)/\omega|$ is larger than δ and monotonically and rapidly increasing when $|(s - s_l)/\omega|$ is smaller than δ. Because of $s - s_l < 0$ (since our truck follows the leading vehicle), the function Φ_2 can be introduced as follows:

$$\Phi_2\left(\frac{s - s_l}{\omega}\right) = \begin{cases} -1 - \delta\dfrac{\omega}{s - s_l}, & \text{if } \dfrac{s - s_l}{\omega} < -\delta \\ 0, & \text{otherwise} \end{cases}$$

where δ is the minimum headway distance allowed between the trucks (see Fig. 11).

This control design ensures that normally the speed control is accomplished with the compression brake but if $|(s - s_l)/\omega|$ becomes smaller than δ, a high gain braking action is produced and both the compression brake and friction brake are engaged to prevent the collision.

The idea of the simulation scenario is that the leading vehicle decelerates to $0.5v_d$ at $t = 5$ s and then accelerates again to v_d at $t = 10$ s. We want to maintain the desired speed 31.6 km/h, and to be sure that our vehicle will not collide with the decelerating leading vehicle. The minimum distance is $\delta = 10$ s (corresponding to $\delta_1 = 0.56$) is allowed. The responses are shown in Figs. 12 and 13. It can be seen from the plot that the position trajectory of the following truck never exceeds the position trajectory of the leading vehicle. This implies that the controller prevented the collision. Note that the friction brakes are engaged when compression brake saturates to provide sufficient braking power.

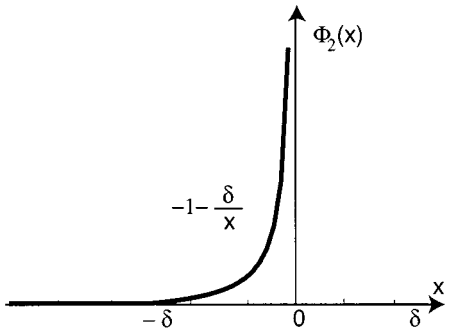

Fig. 11. Barrier function for "vehicle-following" maneuver.

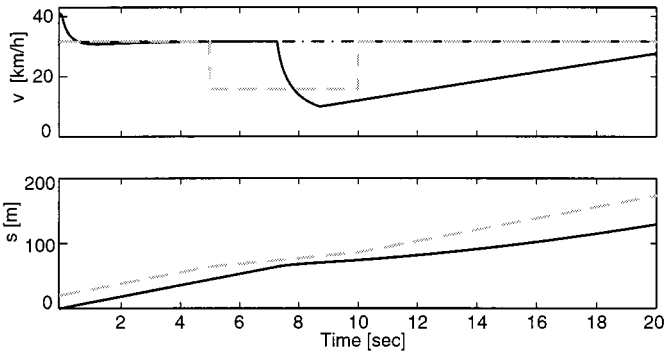

Fig. 12. The engine speed, vehicle speed, vehicle position during vehicle-following maneuver (solid lines). The dash-dotted line shows the desired engine and vehicle speeds while the dashed lines show the vehicle and position trajectory of the leading vehicle.

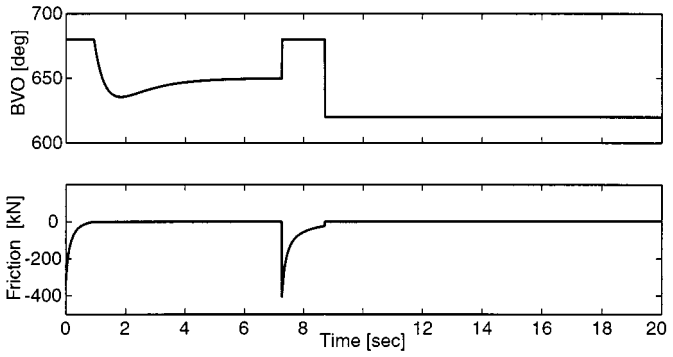

Fig. 13. BVO timing and friction force during vehicle-following maneuver.

VII. Conclusion

Retarding power and retarding control are critical in accommodating higher operational speed and acceleration performance of modern HDVs. They are also fundamental requirements in achieving increased highway capacity and enhanced driving safety which are the major goals of AHS. The use of compression braking in coordination with the conventional friction brakes increases the overall retarding power of the vehicle and lowers maintenance costs on the conventional friction brakes. The compression brake can be used continuously without danger of damage and overheating and it is, thus, a natural actuator to be used for speed control.

In this paper we developed nonlinear SG controllers to accomplish both noncritical and critical longitudinal speed control maneuvers, including traffic constraints. Two ways to handle the

uncertainty in the road grade have been explored, one through the use of an integral action of the SG-PI controller for constant (but unknown) grade, and another one through the differential action of the SG-PD controller for time-varying grade. For large grade or desired vehicle speed changes, we proposed a controller that coordinates the compression brake with the gear ratio adjustment for noncritical maneuvers and also with the friction brakes during the critical maneuvers. In order to avoid excessive friction brake wear, the desired pattern of the braking is maintained whereby the compression brake is used continuously while the friction brake is engaged only when necessary during critical maneuvers. The aggressive maneuver requirements have been handled through the use of the barrier functions within the SG design approach. Simulations results demonstrated good response properties of the controllers.

REFERENCES

[1] J. C. Gerdes, A. S. Brown, and J. K. Hedrick, "Brake system modeling for vehicle control," in *Proc. Advanced Auto. Technol. 1995 ASME IMECE*, pp. 105–112.

[2] J. W. Fitch, *Motor Truck Engineering Handbook*. Warrendale, PA: SAE, 1994.

[3] P. Ioannou and C. C. Chien, "Autonomous intelligent cruise control," *IEEE Trans. Veh. Technol.*, vol. 42, pp. 657–672, 1993.

[4] P. Ioannou and Z. Xu, "Throttle and brake control systems for automatic vehicle following,", PATH Res. Rep. UCB-ITS-PRR-94-10, 1994.

[5] D. B. Maciuca and J. K. Hedrick, "Nonsmooth estimation and adaptive control with application to automotive brake torque," in *Proc. Amer. Contr. Conf.*, 1998, pp. 2253–2257.

[6] D. Yanakiev and I. Kanellakopoulos, "Longitudinal control of automated CHVs with significant actuator delays," in *Proc. 36th Conf. Decision Contr.*, San Diego, CA, 1997, pp. 4756–4763.

[7] S. Chakraborty, T. Gee, and D. Smedley, "Advansed collision avoidance demonstration for heavy duty vehicles," in *SAE Paper 96195*, 1996.

[8] H. Fritz, "Longitudinal and lateral control of heavy duty trucks for automated vehicle following in mixed traffic: Experimental results from CHAUFFEUR project," in *Proc. 1999 IEEE Int. Conf. Contr. Applicat.*, 1999, pp. 1348–1352.

[9] D. D. Cummins, "The Jacobs engine brake application and performance," in *SAE Paper 66-0740*, 1966.

[10] Jacobs Vehicle System. (1999) Intebrake engine braking system for Signature 600. [Online]. Available: http://www.jakebrake.com/products/engine

[11] A. L. Fradkov, "Speed-Gradient scheme in adaptive control," *Automat. Remote Contr.*, vol. 40, no. 9, pp. 1333–1342, 1979.

[12] A. L. Fradkov and A. Yu. Pogromsky, *Introduction to Control of Oscillations and Chaos*. Singapore: World Scientific, 1999.

[13] J. Guldner and V. I. Utkin, "Sliding mode control for gradient tracking and robot navigation using artificial potential fields," *IEEE Trans. Robot. Automat.*, vol. 11, pp. 247–254, 1995.

[14] H. Hu, M. A. Israel, and J. M. Vorih, "Variable valve actuation and diesel engine retarding performance," in *SAE Paper 97-0342*, 1997.

[15] L. Moklegaard, A. Stefanopoulou, and J. Schmidt, "Transition from combustion to variable compression braking," in *SAE Paper 2000-1-1228*.

[16] L. Moklegaard, M. Druzhinina, and A. Stefanopoulou, "Brake valve timing and fuel injection: A unified engine torque actuator for heavy-duty vehicles," in *Proc. 5th Int. Symp. Advanced Vehicle Control*, Ann Arbor, MI, 2000.

[17] R. Sepulchre, M. Jankovic, and P. Kokotovic, *Constructive Nonlinear Control*. New York: Springer-Verlag, 1997.

[18] I. Kolmanovsky, M. Druzhinina, and J. Sun, "Nonlinear torque and air-to-fuel ratio controller for direct injection stratified charge gasoline engines," in *Proc. 5th Int. Symp. Advanced Veh. Contr.*, Ann Arbor, MI, 2000.

[19] M. Druzhinina, L. Moklegaard, and A. Stefanopoulou, "Compression braking control for heavy-duty vehicles," in *Proc. 2000 Amer. Contr. Conf.*, Chicago, IL, 2000.

[20] A. Stotsky and I. Kolmanovsky, "Simple unknown estimation techniques for automotive applications," in *Proc. Amer. Contr. Conf.*, Arlington, VA, June 2001, pp. 3312–3317.

[21] Y. Tan, A. Robotis, and I. Kanellakopoulos, "Speed control experiments with an automated heavy vehicle," in *Proc. 1999 IEEE Int. Conf. Contr. Applicat.*, 1999, pp. 1353–1358.

[22] D. Yanakiev and I. Kanellakopoulos, "Speed tracking and vehicle follower control design for heavy-duty vehicles," *Vehicle Syst. Dyn.*, vol. 25, pp. 251–276, 1996.

[23] S. E. Shladover *et al.*, "Automatic vehicle control developements in the PATH Program," *IEEE Trans. Veh. Technol.*, vol. 40, pp. 114–130, Mar. 1991.

[24] C. Chen and M. Tomizuka, "Steering and independent braking control for tractor-semitrailer vehicles in automated highway systems," in *Proc. 34th IEEE Conf. Decision Contr.*, 1995, pp. 658–663.

Maria Druzhinina received the M.S. degree in applied mathematics in 1992 and the Ph.D. degree in mathematical cybernetics in 1998, both from St. Petersburg State University, Russia.

Since 1992, she has been with the Control of Complex Systems Laboratory of the Institute for Problems of Mechanical Engineering, Russian Academy of Sciences in St. Petersburg. She has held visiting research positions in the Powertrain Control Systems Department of Ford Research Laboratory, Ford Motor Company, in 1999 and in the Mechanical and Environmental Engineering Department of the University of California, Santa Barbara, from 1999 to 2000. She is currently a Research Fellow at the Mechanical Engineering Department of the University of Michigan. Her research interests include nonlinear and adaptive control theory and applications to vehicle and powertrain dynamics, control, and estimation.

Anna G. Stefanopoulou (S'93–M'96) received the Diploma degree in 1991 from the National Technical University of Athens, Athens, Greece, and the M.S. degree in naval architecture and marine engineering from the University of Michigan, Ann Arbor, in 1992. She received the second M.S. degree and the Ph.D. degree in electrical engineering and computer science from the University of Michigan in 1994 and 1996, respectively.

She was an Assistant Professor at the University of California, Santa Barbara, and a Technical Specialist at the Scientific Research Laboratories at Ford Motor Company. She is presently an Associate Professor at the Mechanical Engineering Department at the University of Michigan. Her current research interests include powertrain modeling and control, controller architectures for industrial applications, and multivariable feedback control.

Dr. Stefanopoulou is Chair of the Transportation Panel in ASME DSCD, a recipient of a 1997 NSF CAREER, a 1998–1999 Ford Innovation award, and a 1999/2001 invitee on National Academy of Engineering Symposium on Frontiers of Engineering.

Lasse Moklegaard received the B.S. and M.S. degrees in electrical and computer engineering from the University of California, Santa Barbara, in 1997 and 1999, respectively. He is currently pursuing the Ph.D. degree in the Department of Mechanical and Environmental Engineering at the same university.

His research is on powertrain modeling and control.